Available online at www.sciencedirect.com
SCIENCE DIRECT®
ELSEVIER
Physics and Chemistry of the Earth 29 (2004) 559–567
PHYSICS and CHEMISTRY of the EARTH
www.elsevier.com/locate/pce

On the origin of low- and middler-latitude ionospheric turbulence

O.A. Molchanov

Institute of the Earth Physics, Russian Academy of Sciences, Bolshaya Gruzinskaya 10, 123995 Moscow, Russia

Received 30 May 2003; received in revised form 29 October 2003; accepted 11 November 2003

Abstract

The paper is motivated by our recent results of observation on the satellites Cosmos-900, Aureol-3 and Intercosmos-24, which are presented in this issue (Molchanov et al.). We try to show that a drift mode leading to the ionospheric turbulence (IT) is sustained by wind of the neutral particles, that a source of the IT is energy flux from the atmospheric gravity waves (AGW) to the long scales of IT, and that IT develops to smaller scales as in the classic Kolmogorov's turbulence. Then the earthquake influence observed can be explained by redistribution of the AGW pumping during periods of seismic activity.
© 2004 Published by Elsevier Ltd.

1. Introduction

Oscillating irregularities of the plasma density ($\delta n = n(\mathbf{r}, t) - n_0$) and fluctuations of the electric field ($\mathbf{e} = \mathbf{E}(\mathbf{r}, t) - \mathbf{E}_0$) (where n_0 and $\mathbf{E}_0$ are the averaged values) are observed in the ionosphere, using both traditional ionospheric sounding (so-called F-spread effect) or scintillation technique or radars from the ground and rocket or satellite recordings (Kelley, 1989; Basu et al., 1981; Fejer, 1997; Hysell, 2000, see also a review by Molchanov et al., 2002). We are mainly interested in such events at low- and mid-latitude ionosphere. Spatial scales L of the density irregularities are distributed in a wide range from a tenths of meter to hundreds kilometers. Kelley (1985) states that there are several spatial regimes: long ($L > 20$ km), intermediate ($L = 20$ km–100 m), transitional ($L = 100$–10 m), and short (L from 10 up to 0.1 m).

Interpretation of these phenomena is usually produced in terms of one or other type of plasma instability. For example, the long ionospheric plasma perturbations which can be large (so-called bubbles, $\delta n/n_0 \sim 1$), are explained by gravitational Rayleigh–Taylor (RT) instability. Its linear growth rate γ_1 is positive when the density gradient ∇n is perpendicular to the direction of magnetic field ($\nabla n\mathbf{B} = 0$) and both the directions of ∇n and gravitational force are opposite (Ossakow, 1981). When assuming a conventional vertically dependent ionospheric profile ($\nabla n = \nabla n_z$), the above condition is satisfied only in a region near the magnetic equator below F-layer maximum (height $z \leqslant 350$ km). Such an analysis shows only a possibility of vertical plasma oscillation. For wave-like propagation of these oscillations we need to define their horizontal scale, i.e. to suppose some external wave influence. There is a common consensus that this wave is atmospheric gravity wave (AGW) from the underlying atmosphere (Kelley et al., 1981; Kelley, 1989). That is why Huang and Kelley (1996a,b) performed non-linear computations of the bubble development and its upwelling from the lower into the middle ionosphere on the supposition of AGW as a ''seeding'' wave. Generation of large-scale irregularities in the mid-latitude ionosphere is usually explained in terms of the generalised Rayleigh–Taylor instability (GRT), whose growth rate γ_1 depends not only on ∇n_z but also on the value and direction of quasi-steady electric field $\mathbf{E_0}$. Initiation by AGW should also be supposed in this case (Huang et al., 1998). Special attention was paid to the dependence of resultant power density variation on wave number k ($k \sim 1/L$) in a form $\sim k^{-b}$. Keskinen et al. (1981) and Keskinen and Ossakow (1982) found $1.7 \leqslant b \leqslant 2.5$ both in the equatorial and polar ionospheres.

Efficiency of both the RT and GRT instabilities seems to decrease in the range of intermediate scale due to the diffusion of plasma perpendicular to $\mathbf{B}$ direction. A general approach is to introduce gradient-driven

E-mail address: oleg@uipe-ras.scgis.ru (O.A. Molchanov).

1474-7065/$ - see front matter © 2004 Published by Elsevier Ltd.
doi:10.1016/j.pce.2003.11.018

instabilities, which are lumped under the generic name "drift waves" (Kelley, 1989). The driven mechanism of the intermediate scale irregularities is thought to be the GRT instability, which involves driving agencies such as gravity, electric fields, zonal winds in the presence of tilted ionosphere and vertical winds (Sekar and Kelley, 1998). The smaller scale disturbances are either the drift modes, which are produced in the steep density gradient regions set up by the GRT instability (Ossakow, 1981), or damped modes coupled to large-scale disturbances through a three-wave process (Hysell, 2000). Sudan and Keskinen (1984) and LaBelle et al. (1986) consider non-linear stabilization of the gradient-driven instability and they found spectral indices $b \sim 8/3$.

The drift instability can be extended up to small scales of the order of ion Larmor radius ρ_i. Costa and Kelley (1978) found that the steep gradients are unstable to drift waves which have a peak growth rate of $\gamma \sim 1$ s^{-1} at $k_\perp \rho_i \sim 1.5$. Huba and Ossakow (1979, 1981) and Sperling and Goldman (1980) extended the theory so as to include collisions and shorter-wavelength lower hybrid drift (LHR) modes.

With exception of exotic case of the classic RT instability there is close coupling of the density and electric field variations. They are usually represented by a set of plane waves $\sim \exp(-i\omega t + i\mathbf{kr} + \psi_\mathbf{k})$ (**k** is wave number) and if the phase $\psi_\mathbf{k}$ is a random value, then such a variation is called as turbulence. General properties of the turbulence were intensively considered by laboratory plasma specialists in relation to the problem of controlled nuclear reaction (Kadomtsev, 1964; Tsitovich, 1967). It was found that in a case of weak turbulence there is the same dispersion relationship $\omega = \omega_j(\mathbf{k})$ as for small signals (j is the number of eigenmode). In the usual scenario growth of the turbulence leads to some instability of slow quasi-electrostatic modes, in which the group velocity $\mathbf{V}_g = \partial\omega/\partial\mathbf{k} \approx 0$ and stabilization of well-developed turbulence is due to inter-mode or intra-mode non-linear energy transfer. It is similar to the above-mentioned papers on the ionospheric plasma density–electric field variations.

We try to develop a little bit different concept and show that the drift mode leading to the IT is sustained by wind of the neutral particles (Section 2), that a source of the IT is energy flux from AGW to the long scales of IT (Section 3), and that IT develops to smaller scales as in the classic Kolmogorov's turbulence if the condition of equivalent Reynolds number is valid (Section 4). We have made such an approach, being motivated by recent results which are presented in the companion papers by Molchanov et al. (2003) and by Hobara et al. (in press). Using the data from satellites Cosmos-900, Aureol-3 and Intercosmos-24 they show that k-distribution of the ionospheric density turbulence is nearly the same in a large range of spatial scales from hundreds km to a few meters and that the turbulence intensity correlates definitely with appearance of the electron density Equatorial Anomaly (EA).

2. Eigenmodes in the ionosphere with wind

From the turbulence definition we have $\langle \delta n_m \rangle = \langle \mathbf{e} \rangle = 0$, ($m$ is an index of charged particles) and only power intensity of the electric field variation E_{jk} or $\delta n_m^2/n_{0m}^2$ have a meaning. In particular:

$$\langle \mathbf{e}^2 \rangle = \int E(\omega, \mathbf{k})\, d\omega\, d\mathbf{k} = \sum_j \int E_{jk}(\omega_j(\mathbf{k}))\, d\mathbf{k} \tag{1}$$

We assume the followings:

A1. The external magnetic field $\mathbf{B}_0$ is directed along the axis z and magnetic field turbulence is negligible, $|\mathbf{b}^2|^{1/2} \ll B_0$.

A2. Stable wind of the neutrals with velocity $\mathbf{V}_n$ is directed along the axis **y**, i.e. $(\mathbf{V}_n\mathbf{B_0}) = \mathbf{0}$ and there is a slow variation $V_n(x)$ with large scale $L_{0V} = (\partial \ln V_n/\partial x)^{-1} = \chi_0^{-1}$.

A3. Three particle species: electrons ($m = e$), ions ($m = i$) and neutrals ($m = n$), are considered with single charge (charge $q_i = -q_e = q$). Furthermore we consider low frequencies ($\omega \leqslant \omega_{ci}$ (ion cyclotron frequency)), i.e. we suppose quasi-neutrality of the charged particles:

$$n_e = n_i = n \tag{2}$$

A4. Turbulent variations of the density and electric field are smaller than the quasi-stationary variations (e.g., $n = n_0 + \delta n$, $v_n = V_n + \delta v_n$ and so on, $\delta n \ll n_0$, $\delta v_n \ll V_n$), that allows us to linearize the equations.

A5. Plasma is homogeneous along the **y**, and so we can suppose

$$\partial/\partial y \sim k_y = 0 \tag{3}$$

and suggest that the stationary variations of plasma conductivity, n and V_n depend only on z in the near-polar configuration or on x in the near-equatorial configuration with some characteristic large scale L_0 (e.g., $L_{0V} = (\partial \ln V_n/\partial x)^{-1} = \chi_{0v}^{-1}$ and $L_{0n} = (\partial \ln n_0/\partial x)^{-1} = \chi_{0n}^{-1}$ in the near-equatorial configuration).

A6. Spatial scale of the turbulent variations is smaller than L_0, i.e. for them $\partial/\partial x \approx ik_x$, $\partial/\partial z \approx ik_z$. It leads to the following limitation $|k| > \chi_0 \sim 10^{-6}$–$10^{-5}$ m^{-1}, and to some additional conditions on k_x, k_z. By these assumptions and in linear approximation we have from Maxwell's equations:

$$
\begin{aligned}
&(\partial^2/\partial z^2 + r_{xx})e_x + r_{xy}e_y - \mathrm{i}k\partial e_z/\partial_z = -\mathrm{i}\omega\mu j_{sx}\\
&(\partial^2/\partial z^2 - k^2 + r_{rr})e_y + r_{yx}e_x = -\mathrm{i}\omega\mu j_{sy}\\
&(r_{zz} - k^2)e_z = \mathrm{i}k\partial e_x/\partial_z\\
&\mathrm{i}\omega b_x = -\partial e_y/\partial_z \qquad (4)\\
&\mathrm{i}\omega b_y = (\partial e_x/\partial z)r_{zz}/(r_{rr} - k^2)\\
&\omega b_z = k e_y\\
&\hat{r} = \mathrm{i}\omega\mu\hat{\sigma}
\end{aligned}
$$

$$
\begin{aligned}
&\mathrm{i}\omega b_x = -\partial e_y/\partial z\\
&\mathrm{i}\omega b_y = (\partial e_x/\partial z)r_{zz}/(r_{zz} - k^2) \qquad (5)\\
&\omega b_z = k e_y
\end{aligned}
$$

where $\hat{r} = \mathrm{i}\omega\mu\hat{\sigma}$ and $\hat{\sigma}$ is conductivity tensor.

Hence using the relation of $\partial/\partial z = \mathrm{i}k_z$ we find the following dispersion relationship:

$$
\begin{aligned}
D(\omega, k, k_z) = {} & [r_{xx}(1 - k^2/r_{zz}) - k_z^2][r_{yy} - k^2 - k_z^2]\\
& - r_{xy}r_{yx}(1 - k^2/r_{zz}) = 0 \qquad (6)
\end{aligned}
$$

Let us consider the conductivity tensor. By using the conventional definitions and after linearization; when have

$$
\begin{aligned}
&\mathbf{j} = \mathbf{j}_0 + \boldsymbol{\delta}\mathbf{j}\\
&\mathbf{j}_0 = qn_0(\mathbf{V}_\mathrm{i} - \mathbf{V}_\mathrm{e}) \qquad (7)\\
&\boldsymbol{\delta}\mathbf{j} = qn_0[(\boldsymbol{\delta}\mathbf{v}_\mathrm{i} - \boldsymbol{\delta}\mathbf{v}_\mathrm{e}) + (\mathbf{V}_\mathrm{i} - \mathbf{V}_\mathrm{e})\delta n/n_0] = \hat{\boldsymbol{\sigma}}\mathbf{e} + \mathbf{j}_\mathrm{s}
\end{aligned}
$$

where the particle velocity $\mathbf{v} = \mathbf{V} + \delta\mathbf{v}$, $n = n_0 + \delta n$, $\mathbf{V}_\mathrm{i}$, $\mathbf{V}_\mathrm{e}$ are the drift velocities and all the dependencies can be determined easily in the hydrodynamic approximation. Let us start from the continuity equation. It is easy to find that after linearization and for the spectral components (see e.g. Molchanov et al., 2003, submitted) we have

$$
\begin{aligned}
&\nabla(n_0\mathbf{V}_\mathrm{i}) = Q - \alpha n_0^2\\
&\delta n_k/n_0 = (\mathbf{k} - \mathrm{i}\mathbf{k}_0)\delta\mathbf{v}_{k\perp\mathrm{i}}/(\omega_\mathrm{i}' + \mathrm{i}\omega_\mathrm{r}) \qquad (8)
\end{aligned}
$$

where Q is ionization, α is recombination coefficient, $\omega_\mathrm{i}' = \omega - (\mathbf{k}\mathbf{V}_{\mathrm{i}\perp})$, $\mathbf{k}_0 = \nabla_\perp n_0/n_0$ and $\omega_\mathrm{r} = 2\alpha n_0 + (\nabla_\perp\mathbf{V}_\mathrm{i})$. Thus the density variations are related with those ion velocity variations, which are perpendicular to $\mathbf{B}_0$. Then we consider the motion of equations

$$
\begin{aligned}
&\mathrm{d}\mathbf{v}_\mathrm{i}/\mathrm{d}t = q/m_\mathrm{i}(\mathbf{E} + \mathbf{v}_\mathrm{i}\times\mathbf{B}_0) - C_\mathrm{Ti}^2\nabla n/n - \nu_\mathrm{in}(\mathbf{v}_\mathrm{i} - \mathbf{v}_\mathrm{n}) + \mathbf{g}\\
&\mathrm{d}\mathbf{v}_\mathrm{e}/\mathrm{d}t = -q/m_\mathrm{e}(\mathbf{E} + \mathbf{v}_\mathrm{e}\times\mathbf{B}_0) - C_\mathrm{Te}^2\nabla n/n\\
&\qquad - \nu_\mathrm{en}(\mathbf{v}_\mathrm{e} - \mathbf{v}_\mathrm{n}) - \nu_\mathrm{ei}(\mathbf{v}_\mathrm{e} - \mathbf{v}_\mathrm{i}) + \mathbf{g} \qquad (9)
\end{aligned}
$$

where an isothermal plasma is assumed, C_Te, C_Ti are the thermal velocities, and ν_in, ν_en, ν_ei are the collision frequencies. In a stationary state, we have $(\mathbf{E}_0\mathbf{B}_0) = 0$, $(\nabla n_0\mathbf{B}_0) = 0$, hence the drift velocities are perpendicular to $\mathbf{B}_0$ and we have the following equations:

$$
\begin{aligned}
&\mathbf{V}_\mathrm{i} = X_{\mathrm{i}0}\mathbf{f}_\mathrm{i}/(1 + X_{\mathrm{i}0}^2) + (\mathbf{f}_\mathrm{i}\times\mathbf{B}_0/B_0)/(1 + X_{\mathrm{i}0}^2)\\
&\quad = \widehat{M}_{\mathrm{i}0,\perp}(\mathbf{f}_\mathrm{i}B_0)\\
&\mathbf{f}_\mathrm{i} = \mathbf{E}_0/B_0 - C_\mathrm{Ti}^2\nabla n_0/(n_0\omega_\mathrm{ci}) + \mathbf{g}/\omega_\mathrm{ci} + X_{\mathrm{i}0}\mathbf{V}_\mathrm{n}\\
&X_{\mathrm{i}0} = \nu_\mathrm{in}/\omega_\mathrm{ci} \qquad (10)\\
&\mathbf{V}_\mathrm{e} = \widehat{M}_{\mathrm{e}0,\perp}(\mathbf{f}_\mathrm{e}B_0)\\
&\mathbf{f}_\mathrm{e} = \mathbf{E}_0/B_0 - C_\mathrm{Te}^2\nabla n_0/(n_0\omega_\mathrm{ce})\\
&\qquad + \mathbf{g}/\omega_\mathrm{ce} + X_{\mathrm{e}0}\mathbf{V}_\mathrm{n} + (\nu_\mathrm{ei}/\omega_\mathrm{ce})\mathbf{V}_\mathrm{i}\\
&X_{\mathrm{e}0} = \nu_\mathrm{en}/\omega_\mathrm{ce} \ll X_{\mathrm{i}0}, 1
\end{aligned}
$$

where $\widehat{M}_{\mathrm{i}0,\mathrm{e}0}$ are the stationary mobility tensors of ions and electrons. In the lower ionosphere (altitudes 90 km $< h <$ 200 km; $X_{\mathrm{i}0} > 0.05$) we can neglect gradient and gravitational terms in $\mathbf{f}_\mathrm{i}$, and the last three terms in $\mathbf{f}_\mathrm{e}$ if $V_\mathrm{n} \geqslant 10$ m/s. This value is indeed larger and we suppose $V_\mathrm{n} \sim 100$ m/s. Hence: $\mathbf{f}_\mathrm{i} \approx \mathbf{E}_0/B_0 + X_{\mathrm{i}0}\mathbf{V}_\mathrm{n}$ and $\mathbf{f}_\mathrm{e} \approx \mathbf{E}_0/B_0$. In the absence of $\mathbf{E}_0$:

$$
\begin{aligned}
&\mathbf{V}_\mathrm{i} = X_{\mathrm{i}0}^2\mathbf{V}_\mathrm{n}/(1 + X_{\mathrm{i}0}^2) + (\mathbf{V}_\mathrm{n}\times\mathbf{B}_0/B_0)X_{\mathrm{i}0}/(1 + X_{\mathrm{i}0}^2)\\
&\mathbf{V}_\mathrm{e} \sim 0 \qquad (11)
\end{aligned}
$$

Thus an effect of the ion entrainment appears, which is maximal at $h \sim 150$ km when $X_{\mathrm{i}0} \sim 1$ and $V_\mathrm{i} \sim V_\mathrm{n}$.

As concerned with the velocity variations we have, from (9), the spectral components:

$$
\begin{aligned}
&\delta\mathbf{v}_\mathrm{i} = \widehat{M}_\mathrm{i}(\mathbf{e} + \mathbf{e}_\mathrm{wi})\\
&\delta\mathbf{v}_\mathrm{e} = \widehat{M}_\mathrm{e}(\mathbf{e} - \nu_\mathrm{ei}B_0\widehat{M}_\mathrm{i}(\mathbf{e})/\omega_\mathrm{ce} - \mathbf{e}_\mathrm{we}) \qquad (12)
\end{aligned}
$$

where remembering that $k_y = 0$

$$
\begin{aligned}
&M_{\mathrm{i(e)},xx} = \pm X_{\mathrm{i(e)}}/[B_0(1 + X_{\mathrm{i(e)}}X_{\mathrm{i(e)}}')]\\
&M_{\mathrm{i(e)},xy} = -M_{\mathrm{i(e)},yx} = 1//[B_0(1 + X_{\mathrm{i(e)}}X_{\mathrm{i(e)}}')]\\
&M_{\mathrm{i(e)},yy} = \pm X_{\mathrm{i(e)}}'/[B_0(1 + X_{\mathrm{i(e)}}X_{\mathrm{i(e)}}')]\\
&M_{\mathrm{i(e)},zz} = \pm 1/(B_0X_{\mathrm{i(e)},z}')\\
&M_{\mathrm{i(e)},xz} = M_{\mathrm{i(e)},zx} = M_{\mathrm{i(e)},yz} = M_{\mathrm{i(e)},zy} = 0\\
&X_{\mathrm{i(e)}} = (\nu_{\mathrm{i(e)}} - \mathrm{i}\omega_{\mathrm{i(e)}}')/\omega_{\mathrm{ci(ce)}}\\
&X_{\mathrm{i(e)}}' = X_{\mathrm{i(e)}} + \mathrm{i}d_{\mathrm{i(e)}}\\
&X_{\mathrm{i(e)},z} = X_{\mathrm{i(e)}} + \mathrm{i}d_{\mathrm{i(e)},z}\\
&\omega_{\mathrm{i(e)}}' = \omega - kV_{\mathrm{i(e)},x}\\
&d_{\mathrm{i(e)}} = kC_{\mathrm{Ti(e)}}^2/[\omega_{\mathrm{ci(ce)}}u]\\
&d_{\mathrm{i(e)},z} = (k_z/k)d_{\mathrm{i(e)}}\\
&\nu_\mathrm{i} = \nu_\mathrm{in}\\
&\nu_\mathrm{e} = \nu_\mathrm{en} + \nu_\mathrm{ei}\\
&u = (\omega_\mathrm{i}' + \mathrm{i}\omega_\mathrm{r})/(k - \mathrm{i}k_0)
\end{aligned}
$$

and $\mathbf{e}_\mathrm{wi} = (\nu_\mathrm{in}B_0/\omega_\mathrm{ci})\delta\mathbf{v}_\mathrm{n}; \mathbf{e}_\mathrm{we} = (\nu_\mathrm{en}B_0/\omega_\mathrm{ce})\delta\mathbf{v}_\mathrm{n} + (\nu_\mathrm{ei}B_0/\omega_\mathrm{ce})\widehat{M}_\mathrm{i}(\mathbf{e}_\mathrm{wi})$.

It is easy to find the followings:

$$\begin{aligned}\hat{\sigma}\mathbf{e} &= qn\Big\{[\widehat{M}_{\rm i}(\mathbf{e}) - \widehat{M}_{\rm e}(\mathbf{e} - v_{\rm ei}B_0\widehat{M}_{\rm i}(\mathbf{e})/\omega_{\rm ce})] \\ &\quad + (\mathbf{V}_{\rm i} - \mathbf{V}_{\rm e})\widehat{M}_{\rm ix}(\mathbf{e})/u\Big\} \\ \mathbf{j}_{\rm s} &= qn_0\Big\{[\widehat{M}_{\rm i}(\mathbf{e}_{\rm wi}) + \widehat{M}_{\rm e}(\mathbf{e}_{\rm we})] \\ &\quad + (\mathbf{V}_{\rm i} - \mathbf{V}_{\rm e})\widehat{M}_{\rm ix}(\mathbf{e}_{\rm wi})/u\Big\}\end{aligned} \tag{13}$$

Supposing $v_{\rm i}/\omega_{\rm ci} \gg v_{\rm e}/\omega_{\rm ce}$ that is valid for $h < 300$ km and taking into consideration of $|X|_{\rm i} \gg |X_{\rm e}|$, we simplify Eq. (13) as follows:

$$\begin{aligned}&\sigma_{xx} = \varepsilon_0 pX_{\rm i}(1 + \Delta V_x/u)/(1 + X_{\rm i}'X_{\rm i}) \\ &\sigma_{xy} = \varepsilon_0 p(-X_{\rm i}'X_{\rm i} + \Delta V_x/u)/(1 + X_{\rm i}'X_{\rm i}) \\ &\sigma_{yx} = \varepsilon_0 pX_{\rm i}(X_{\rm i}' + \Delta V_y/u)/(1 + X_{\rm i}'X_{\rm i}) \\ &\sigma_{yy} = \varepsilon_0 p(X_{\rm i}' + \Delta V_y/u)/(1 + X_{\rm i}'X_{\rm i}) \\ &\sigma_{zz} = \varepsilon_0 p/X_{e,z}' \\ &\Delta\vec{V} = \vec{V}_{\rm i} - \vec{V}_{\rm e} \\ &p = qn_0/(\varepsilon_0 B_0) = \omega_{pe}^2/\omega_{\rm ce} \\ &j_{\rm sx} = qn_0 v_{\rm in}/[\omega_{\rm ci}(1 + X_{\rm i}'X_{\rm i})]\{(X_{\rm i} + \Delta V_x/u)\delta v_{\rm nx} \\ &\qquad + (1 + \Delta V_x/u)\delta v_{\rm ny}\} \\ &j_{\rm sy} = qn_0 v_{\rm in}/[\omega_{\rm ci}(1 + X_{\rm i}'X_{\rm i})]\{(X_{\rm i}\Delta V_y/u - 1)\delta v_{\rm nx} \\ &\qquad + (X_{\rm i}' + \Delta V_y/u)\delta v_{\rm ny}\}\end{aligned} \tag{14}$$

In the absence of wind and in the cold plasma approximation ($d_{\rm i(e)} = 0$) it reduces to the well-known following relations

$$\begin{aligned}&\sigma_{xx}^r = \sigma_{yy}^r = \sigma_P = \varepsilon_0 pX_{\rm i}/(1 + X_{\rm i}^2) \\ &\sigma_{xy}^r = -\sigma_{yx}^r = \sigma_H = -\varepsilon_0 pX_{\rm i}^2/(1 + X_{\rm i}^2) = -\sigma_P X_{\rm i} \\ &\sigma_{zz}^r = \sigma_z = \varepsilon_0 p/X_{\rm e} \\ &\mathbf{j}_{\rm s} = 0\end{aligned} \tag{15}$$

where $X_{\rm i(e)} = (v_{\rm i(e)} - i\omega_{\rm i(e)})/\omega_{\rm ci(ce)}$ and the dispersion relationship (6) takes the following equation:

$$\begin{aligned}D^r(\omega, k, k_z) &= [r_P(1 - k^2/r_z) - k_z^2][r_P - k^2 - k_z^2] \\ &\quad + r_H^2(1 - k^2/r_z) = 0\end{aligned}$$

where the connection of the coefficients with conductivity tensor is the same as in (5).

There are two modes of propagation in this case

$$\begin{aligned}k_{z,\pm}^2 &= r_P - k^2/2(1 + r_P/r_z) \pm \big[k^4/4(1 - r_P/r_z) \\ &\quad - r_H^2(1 - k^2/r_z)\big]^{1/2}\end{aligned} \tag{16}$$

which are on the usual assumptions:

$$r_P \ll r_z; k^2 \ll |r_z| = (\omega_{pe}^2/c^2)|\omega/(v_{\rm e} - {\rm i}\omega)| \tag{17}$$

can be presented as follows:

$$k_{z,\pm}^2 = k_{\rm A}^2 - k^2/2 \pm [k^4 - k_{\rm A}^4 X_{\rm i}^2]^{1/2}$$

where $k_{\rm A}^2 = {\rm i}\omega\mu\sigma_P = \omega(\omega + {\rm i}v_{\rm i})/[c_{\rm A}^2(1 + X_{\rm i}^2)]$ and $c_{\rm A} = c\omega_{\rm ci}/\omega_{\rm pi}$ is the conventional Alfven velocity. The first mode corresponds to the known Alfven mode in the collisionless plasma and the second is isotropic or fast magneto-sonic mode. As for a problem of mode generation the dispersion relationship in the approximation often used,

$$k_z/k = a \ll 1 \tag{18}$$

can be rewritten as follows:

$$\begin{aligned}\omega_+ &= [c_{\rm A}^2(1 + v_{\rm i}^2/\omega_{\rm ci}^2)k_z^2 - v_{\rm i}^2/4]^{1/2} - {\rm i}v_{\rm i}/2 \\ \omega_- &= [c_{\rm A}^2 k^2 - v_{\rm i}^2/4]^{1/2} - {\rm i}v_{\rm i}/2\end{aligned} \tag{19}$$

where the cut-off k-values and attenuation coefficients are evident.

$$\begin{aligned}&k_-^* = v_{\rm i}/2c_{\rm A} \\ &k_+^* = v_{\rm i}/2c_{\rm A}[a^2(1 + v_{\rm i}^2/\omega_{\rm ci}^2)]^{-1/2} > k_-^* \\ &\gamma_\pm = {\rm Im}(\omega_\pm) = \begin{matrix}-(v_{\rm i}/4)k^2/k_\pm^{2\,*} & k \ll k_\pm^* \\ -(v_{\rm i}/2) & k \ll k_\pm^*\end{matrix}\end{aligned}$$

The situation is depicted in Fig. 1a.

In a case of wind-induced plasma we need to investigate the more complicated dispersion relationship with substitution of the relations (14). It is obvious that a new drift mode appears:

$$\omega = \omega_{\rm d} \approx kV_{\rm ix} - {\rm i}\gamma_{\rm d} \tag{20}$$

where, after simple estimation

$$\begin{aligned}\gamma_{\rm d} &\approx \omega_{\rm r} - v_{\rm i}(V_{\rm ix} - V_{\rm ex})^2/(c_{\rm A}a)^2 \\ &\approx 2\alpha n_0 + \partial V_{\rm ix}/\partial x - v_{\rm i}(V_{\rm ix} - V_{\rm ex})^2/(c_{\rm A}a)^2\end{aligned} \tag{21}$$

Taking into consideration $\partial V_{\rm ix}/\partial x < 0$ in the low-latitude ionosphere, it is evident now that this mode could be weekly attenuated or even unstable ($\gamma_{\rm d}(x) < 0$) at the altitude range 150 km $< h <$ 250 km. At these altitudes $v_{\rm i} \sim 1$–$100\ {\rm s}^{-1} < \omega_{\rm ci}$, $c_{\rm A} \sim 100$–300 km/s and $k_-^* \sim 10^{-5}$–$10^{-4}\ {\rm m}^{-1}$, but $k_+^* \sim 10^{-4}$–$10^{-3}\ {\rm m}^{-1}$. The new situation and a possibility of mode coupling is schematically depicted in Fig. 1b. Note that frequency range of the drift mode before coupling is $\omega_{\rm d} \sim 10^{-2}$–$10^{-3}$ Hz that corresponds to the periods of $\tau \sim 10$–100 min. It is just a range of the gravity waves in the atmosphere.

3. Pumping of ionospheric turbulence by gravity waves

Using the conventional axis system $\mathbf{z}//\mathbf{g}$, $\mathbf{V}_{\rm n}//\mathbf{y}$ in a plane which is perpendicular to the wind direction ($\mathbf{kV_n} = 0$), the dispersion relation for GW ($\omega \leqslant \omega_{\rm g}$, here $\omega_{\rm g}$ is Brant–Vaisala frequency) is given by (Hines, 1974),

$$k_x^2(1/x^2 - 1) = k_z^2 + k_0^2(b_{\rm a} - x^2) \tag{22}$$

where $x = \omega/\omega_{\rm g}$, $\omega_{\rm g} = g(\gamma_{\rm a} - 1)^{1/2}/Cs$ and $\gamma_{\rm a}$ is specific heat ratio.

$k_0 = g(\gamma_{\rm a} - 1)^{1/2}/Cs^2 = \omega_{\rm g}/Cs = b_{\rm a}^{1/2}/2Ha$, $Ha = Cs^2/(g\gamma_{\rm a})$ is the well-known atmospheric height and $b_{\rm a} = 0.25\gamma_{\rm a}^2/(\gamma_{\rm a} - 1)$. For two-atomic gases in the atmo-

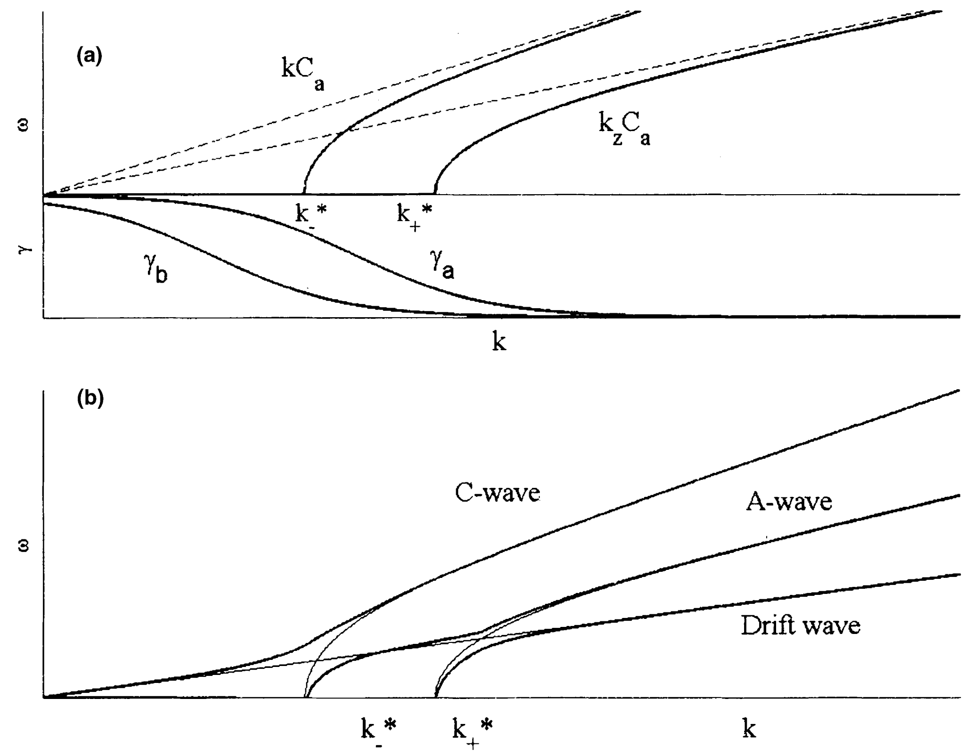

Fig. 1. (a) Dispersion relationship $\omega(k, k_z)$ in the ionospheric cold plasma without wind. On the assumption $k_z/k \leqslant 0.1$ and $X_i \ll 1$ (see text), $\omega \approx k_z C_A$ for Alfven mode and $\omega \approx kC_A$ for compression mode and (b) dispersion curves for the ionospheric plasma with wind of neutral particles. In addition to fast Alfven and compression modes the slow quasi-electrostatic mode appears $\omega \approx kV_{di}$, where V_{di} is drift velocity of the ions.

sphere $\gamma_a = 1.4$ and $b_a = 1.22$. It is evident that the GW propagation depends essentially on the angle between **k** and z-axis ($k_x/k_z = tg\theta$) and there is a resonance cone $\theta = \theta_{res}$ when $k \to \infty$. Near this resonance cone an energy focusing is possible and it is easy to obtain $\sin\theta_{res} = x$. Taking into account that the group velocity $\mathbf{V}_{gr}$ (or direction of GW energy) is perpendicular to the wave vector surface we find almost vertical energy flux for $x \sim 1$ and almost horizontal energy propagation for $x \ll 1$.

Let us consider the GW energy flux into the ionosphere:

$$P_z(\omega) = \langle \Delta p_z \Delta v_z \rangle_\omega = 2\int_{\psi_{res}}^{\pi/2} P_{z\psi}\, d\psi \qquad (23)$$

where Δp_z, Δv_z are the perturbations of pressure and velocity, the averaging is performed over a wave period and the angle of energy propagation defined from the following relation:

$$tg\psi = V_{gr,x}/V_{gr,z} = -tg\theta(1-x^2)/x^2 \qquad (24)$$

The value of GW energy flux depends on the properties of the source. Mareev et al. (2002) have supposed that the source is near the ground with its horizontal size R, thickness H_z and they have considered 1-D turbulence along the x-axis. They have found,

$$\begin{aligned} &P_{z\psi} = P_z(\omega, k_x)\partial k_x^2/\partial\psi \\ &P_z(\omega, k_x) = Ba^2(\omega, k_x) \\ &B = \rho Cs^2\omega_g(\gamma_a - 1)/[\gamma_a^4(1-x^2)^{1/2}] \\ &a^2(\omega, k_x) = \{\delta T^2(\omega, k_x)/T^2 + \delta n^2(\omega, k_x)/n^2\} \end{aligned} \qquad (25)$$

Mareev et al. (2002) have assumed a specific form of correlation inside the source:

$$a^2(\omega, \Delta x_s) = CF(x)/(1 + \Delta x_s^2/L^2)^\eta \qquad (26)$$

where Δx_s is displacement along x-axis in the source, $F(x)$ is frequency distribution, $L = L_x < R$ is internal correlation size and η is fractal number of the turbulence. If we suggest for simplicity $\eta = 1$, then their result is reduced as follows:

$$\begin{aligned} &a^2(\omega, k_x) = a^2(\omega, -k_x) = CF(x)L\exp(-|k_x|L) \\ &P_z(\omega) = 2BCF(x)/L \\ &P_{z\psi} = P_z(\omega)\phi(x, \omega, L) \end{aligned} \qquad (27)$$

where the radiation diagram is as follows:

$$\phi(x, \omega, L) = L^2(\partial k_x^2/2\partial\psi)\exp(-|k_x|L) \qquad (28)$$

and it is normalized ($\int \phi d\psi = 1$).

The constant C can be determined from the conventional relation:

$$\langle a^2(t, \Delta x_s, \Delta y_s, \Delta z_s) \rangle = \int_0^{\omega_g} d\omega \int a^2(\omega, k_x, k_y, k_z) dk_x\, dk_y\, dk_z$$

where $\langle a^2 \rangle$ is the variance of perturbation in the source. In our case 26,27 we find

$$C = L_y L_z \langle a^2 \rangle / (\omega_g A) \approx R H_z \langle a^2 \rangle / (\omega_g A) \tag{29}$$

where $A = \int_0^1 F(x)\,dx$. Hence,

$$P_z(\omega) = 2BF(x)H_z(R/L)\langle a^2 \rangle/(\omega_g A) \sim (\rho Cs^2 F(x)/2)H_z(R/L)\langle a^2 \rangle$$

and total energy flux from the source:

$$P_{zs}(\omega) \sim P_z(\omega)R^2 \sim (\rho Cs^2 F(x)/2)V_s(R/L)\langle a^2 \rangle \tag{30}$$

where $V_s \sim R^2 H_z$ is volume of the source.

This result looks as almost obvious. Indeed for a supposed crest-like structure with scale $L \ll R$ and due to the ergodic theorem, we have

$$\langle a^2 \rangle = (1/Vs)\int_{Vs} a^2(\Delta x, \Delta y, \Delta z)\,dVs \approx (N_L a_L^2 LRH_z)/Vs \approx a_L^2$$

where a_L^2 is intensity of the structure's perturbation (fluctuation of L-scale) and $N_L \approx R/L$ is averaged number of the crests. So we have:

$$P_{zs}(\omega) \sim (\rho Cs^2 F(x)/2)V_s N_L a_L^2 \tag{31}$$

In reality there exists the perturbation of different scales. For example, Tramutoli et al. (2001) and Tronin et al. (2002), using the IR satellite data, reported on the appearance of several temperature anomalies with scale $L = 10$–50 km and $\delta T \sim 1$–$2°$ in association with seismic activity. To comply with such data we transform (31) in the following manner:

$$p_{zs}(\omega) \sim P_z^0 R^2$$
$$P_z^0(\omega) \sim (\rho Cs^2 F(x)H_z/2)\sum_{i=1}^{N} a_{Li}^2 \tag{32}$$

where $P_z^0(\omega)$ is power flux per m^2 just above the source and $a_{Li}^2 \approx \delta T^2/T^2 \sim 10^{-5}$.

In order to estimate the flux in the ionosphere we need to take into account its divergence and attenuation during the course of propagation. Mareev et al. (2002) have analyzed the radiation diagram and have found that the radiation maximum is near the resonance cone for $x < 0.9$ and not so large value of L ($k_0 L \sim 1 \sim L/2Ha$).

This diagram is rather narrow and group velocities in the maximum are as follows:

$$V_{gr,z,\max} \approx Cs(k_0 L/2)x^2$$
$$V_{gr,z,\max}/V_{gr,x,\max} \approx x \tag{33}$$

Using the formulas (24), (28) and neglecting viscosity attenuation in the atmosphere the distribution $P_z(\omega)$ at the level of lower ionosphere ($h \sim 100$ km) in the horizontal plane is described by a simple relation:

$$P_z(\omega, l, h) = P_z^0(\omega)2x^2 d^2 \exp[-(l/h - l_c)^2/\Delta l^2]/(D_1^2 - D_2|D_2|)$$

where l is horizontal distance from projection of the source center on the ionospheric plane, $l_c = (1-x^2)^{1/2}/x - q_0 x$ is relative shift of the radiation pattern and $d = R/(2h)$,

$$q_0 \approx (k_0 L)^2(b_a - x^2)/[88(1-x^2)^{1/2}]$$
$$D_1 = (1-x^2)^{1/2} + dx \tag{34}$$
$$D_2 = (1-x^2)^{1/2} - dx - q_0 x^2$$

Examples of the distribution are shown in Fig. 2. It can be seen from the figure that the space–frequency discrimination is performed in the atmosphere and the main impact is expected for frequency range $x = 0.1$–0.9 (periods $T_w \sim 7$–60 min supposing $T_B = Cs/\omega_g \approx 6$ min) and horizontal distances ± 300–1000 km above the source center.

Let us consider finally a matching of GW and electrostatic turbulence in the ionosphere. At first we need to determine the variation of the neutral velocity. It is easy to find the following estimation,

$$\delta v_n(\omega, h, l) \approx P_z(\omega)A\sqrt{\omega_g}/[\rho^0 Cs^2(\delta\rho^0/\rho^0)](\rho^0/\rho)^{1/2} \approx H_z\sqrt{\omega_g}(\delta T/T)^0(P_z(\omega)/P_z^0(\omega))F(x) \times \exp(h/2H_a) \tag{35}$$

where we suppose for simplicity $A \approx 1$ and $(\delta\rho^0/\rho^0) \sim (\delta T/T)^0$ inside the source of GW perturbation. It is known that matching is efficient if there is synchronism between GW and ionospheric turbulence (IT). In a case of plane wave interaction it leads to the condition of phase velocity equality: $V_{ph}(\mathrm{GW}) = V_{ph}(\mathrm{IT})$, but in our case of turbulent interaction it transforms to the following condition for the near-equatorial configuration (see previous section):

$$V_{gr,z}(\omega)_{\mathrm{GW}} = V_i \approx V_n \tag{36}$$

and to other condition for the near-polar configuration:

$$V_{gr,x}(\omega)_{\mathrm{GW}} = V_i \approx V_n \tag{37}$$

Using now the relations (33) we estimate relative frequencies of the synchronism,

$$x^*_{eq} \approx (2V_n/(k_0 LCs))^{1/2}$$
$$x^*_{pol} \approx (2V_n/(k_0 LCs)) \tag{38}$$

As a result the supposing averaged values $V_n \sim 30$–100 m/s, $k_0 LC_s \sim 10^3$ m/s we find that an efficient GW–IT interaction is possible for the frequencies $x^*_{eq} \sim 0.2$–0.4 ($T_w \sim 15$–30 min) in the near-equatorial region and $x^*_{pol} \sim 0.05$–0.2 ($T_w \sim 30$–120 min) in the near-polar configuration, both values are in a range of internal gravity waves. As concerned with δv_n values we have from (35) assuming $H_z \sim 100$ m, $H_a \sim 6$ km and $h \sim 100$

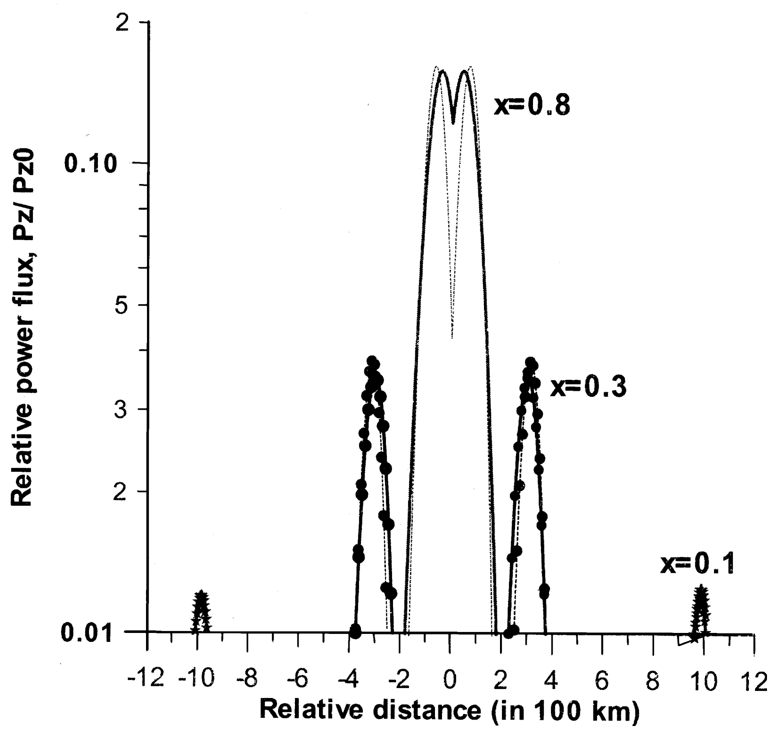

Fig. 2. GW power flux $P_z(\omega)$ at height $h = 100$ km as a ratio to power flux just above the source (height of the upper source boundary $H_z = 100$ m) with dependence on the horizontal distance from the projection of the source center and for different relative frequencies $x = \omega/\omega_g$ where ω_g is Brant–Vaisala frequency. Dash line is for $k_0L = 1$ ($L \sim 12.5$ km) and solid line for $k_0L = 2$ ($L \sim 25$ km).

km, $\delta v_n \sim 3$–5 m/(s$\sqrt{}$Hz) at the near-equatorial region and $\delta v_n \sim 0.1$–0.4 m/(s$\sqrt{}$Hz) in the near-polar region.

4. Development of IT in *k*-space

Now we show that IT *k*-distribution could be understood as a result of cascade non-linear energy transfer from larger scales of the order of 1000 km to smaller scales up to meters, which is similar to the origin of classic hydrodynamic turbulence. Kolmogorov (1941) found that in the following conditions,

(a) Water flux with velocity U exists,
(b) The flux meets the obstacle with size L_0,
(c) Values U, L_0 are so large that Reynolds number $R_v = UL_0/v_v \gg 1$ (where v_v is dynamic viscosity), then the turbulent curls with scales L in a range $L_0 > L > L_{\min}$ appear after the obstacle with special distribution of the curls intensity on L. This distribution represents usually in terms of $k \sim 1/L$ and following the definition of turbulent intensity (variance):

$$\langle \delta U^2 \rangle = \int E_k \, \mathrm{d}k$$

the main result of Kolmogorov's theory is given as follows,

$$E_k \sim k^{-5/3} \text{ in the inertial range } k_0 < k < k_{\max}.$$

The result is well supported by observations, but it has no rigid mathematical proof yet. One of non-rigid (physical) approaches to this explanation is related with the construction of perturbation increment or second order structure function in 1-D approximation (Frisch, 1995):

$$\langle (\delta U(s+L) - \delta U(s))^2 \rangle_s = 2\int_{-\infty}^{\infty} (1 - \exp(ikL))E_k \, \mathrm{d}k \approx \varepsilon_L \tag{39}$$

where the Wiener–Khinchin formula is used

$$E_k = E_k = (1/2\pi)\int_{-\infty}^{\infty} E_k = (1/2\pi)\int_{-\infty}^{\infty} \exp(ikL)\Gamma(L)\, \mathrm{d}L$$

for the correlation function of $\Gamma(L) = \langle \delta U(s+L)\delta U(s) \rangle$.

Thus we find from Eq. (39),

$$\varepsilon_L = 16\int_0^{\infty} \sin^2(kL/2)E_k \, \mathrm{d}k \approx kE_k(k = \pi/L) = \varepsilon_k \approx \delta U_k^2 \tag{40}$$

where ε_L can be named as intensity of perturbation of L-size or k-size, if they are connected as shown in (40). The important fact is that expansion of variance onto a sum of perturbations with different sizes is possible:

$$\langle \delta U^2 \rangle = \sum_{k_0}^{k_{\max}} \varepsilon_k \quad (41)$$

and intensity of each perturbation can be estimated from the power-spectrum distribution in k-space using (40). Then we consider an equation of intensity balance,

$$\mathrm{d}\varepsilon_k/\mathrm{d}t = -\gamma_k \varepsilon_k + \Phi_k + \Psi_k \quad (42)$$

where γ_k is linear decrement of the turbulence dissipation, Φ_k is forcing and Ψ_k is a function of non-linear energy transfer. There are conventional assumptions at this point (Frisch, 1995),

(1) $\gamma_k = -v_v k^2 = -\gamma_1 \sim 0$ in $[k_0, k_m]$ and $\gamma(k > k_m) \gg \gamma_1$. It is an assumption of the the weak attenuation in the inertial range.
(2) $\Phi_k(k_0 < k < k_{\max}) = 0$, but $\Phi_k(k \leqslant 0) = \Phi_0$. It is an assumption on energy pumping to larger scales.
(3) $\Psi_k = S_{k+} - S_{k-}$, where S_{k+} is input energy flux in the ε_k turbulence cell from the neighbor cell $(k_+ < k)$ and S_{k-} is output flux in the cell $k_- > k$. It means that cascade interaction is supposed,

$$(k_- - k_+) \ll k \quad (43)$$

In stationarity, we have

$$S_{k+} = S_{k-} + \gamma_k \varepsilon_k \quad (44)$$

and due to assumption (1)

$$S_{k+} \approx S_{k-} \approx S_k \approx \text{constant} \quad (45)$$

On the other hand using (42) we have

$$\begin{aligned} &\mathrm{d}\varepsilon_k/\mathrm{d}t \approx (\varepsilon_{k+} - \varepsilon_{k-})/\tau_k \approx S_{k+} - S_{k-} \\ &\varepsilon_k/\tau_k \approx S_k \end{aligned} \quad (46)$$

where τ_k is the so-called turn-over time. Finally supposing now $\tau_k \approx L/\delta U_k \approx 1/(k\delta U_k)$ and taking into account (45) and (40) we find,

$$\delta U_k \sim k^{-1/3}, \quad \varepsilon_k \sim k^{-2/3} \quad \text{and} \quad E_k \sim k^{-5/3}$$

The situation with IT is more complicated but there is a definite similarity to the classical one. In a place of above-mentioned classic conditions we have plasma drift with velocity V_d, and instead of laminar flux with velocity U we have the Equatorial Anomaly with basic scale L_0 as a main "obstacle" to the drift. To find an analogy of Reynolds number we need to modify a little its definition as follows:

$$R_v = UL_0/v_v = k^2 UL_0/\gamma_k \approx (kU/\gamma_k)(L_0/L)$$

So at least at the beginning of the cascade process $(L \leqslant L_0)$ the condition $R_v \gg 1$ goes in the plasma to the condition,

$$kV_\mathrm{d} \approx \omega_k \gg \gamma_k$$

that is a trivial condition of efficient non-linear energy transfer. As concerned with the theoretical assumptions the main one is supposition on the cascade interaction or existence of non-linear scattering with $\Delta k \ll k$. This approach was used by Sudan and Keskinen (1984), and they analyzed the equation, which is similar to the one obtained from a combination of (44) and (46)

$$\mathrm{d}(\varepsilon_k/\tau_k)/\mathrm{d}k = \gamma_k \varepsilon_k/\Delta k \quad (47)$$

If we suppose $\tau_k \sim 1/\omega_k \approx (kV_\mathrm{d})^{-1}$ and $(\gamma_k/\Delta k V_\mathrm{d}) \ll 1$ then $E_k \sim k^{-2}$, that more or less corresponds to the observation data on IT.

5. Discussion

Our approach is based on the simple idea: ionospheric turbulence (IT) origin as a result of the conversion of atmospheric gravity waves (AGW) in the lower ionosphere. In regular situation the most effective matching is for large scales $L \sim$ 1000–2000 km that are harmonics of tidal atmospheric oscillations and that produce the pumping of IT near the scale $L_0 \sim 1000$ km (see our relation (46)). Due to non-linear energy transfer in k-space the regular multi-scale IT exists as a permanent phenomenon with fractal values $\sim$ 1.5–2. However, during the periods of seismic activity the AGW pumping in the range of scales tens hundreds km seems to appear (see e.g. the discussion in Mareev et al. (2002) and the results of satellite IR observations in Tramutoli et al. (2001) and Tronin et al. (2002)). This additional pumping can intensify the IT for smaller scales and suppress the IT for larger scales. As a result, redistribution of IT intensity in k-space can be expected. On such a way we need in addition to consider the penetration of IT into the upper ionosphere and the problem of slow electrostatic mode transformation to the fast Alfven and isotropic modes. We hope to present this research later. Note finally that our approach is helpful not only for the explanation of above-mentioned satellite observation results but also for the explanation of some ULF observations on the ground associated with large earthquakes (Molchanov et al., submitted).

Acknowledgements

This research was partially supported by ISTC under Grant 1121 and by Commision of the EU grant No. INTAS-01-0456. The author is thankful for the support from International Space Science Institute ISSI at Bern, Switzerland within the project "Earthquake influence of the ionosphere as evident from satellite density–electric field data".

References

Basu, Su., Basu, Sa., Ganguly, S., Klobuchar, J.A., 1981. Generation of kilometer scale irregularities during the midnight collapse at Aresibo. J. Geophys. Res. 86, 7607.

Costa, C.S., Kelley, M.C., 1978. On the role of steepened structures and drift waves in the equatorial spread F. J. Geophys. Res. 83, 4359–4364.

Fejer, B.G., 1997. The electrodynamics of the low-latitude ionosphere: recent results and future challenges. J. Atmos. Solar-Terr. Phys. 59, 1456–1482.

Frisch, U., 1995. Turbulence. The legacy of A.N. Kolmogorov. Cambridge University Press. 179 p.

Hines, C.O., 1974. The upper atmosphere in motion: a selection of papers with annotation. In: Geophysics Monograph, 18. American Geophysics Union, Washington, DC.

Hobara, Y., Lefeuvre, F., Parrot, M., Molchanov, O.A., in press. Low latitude ionospheric turbulence and possible association with seismicity from satellite Aureol 3 data.

Huang, C.S., Kelley, M.C., 1996a. Nonlinear evolution of equatorial spread F, 1. On the role of plasma instabilities and spatial resonance associated with gravity wave seeding. J. Geophys. Res. 101, 283–292.

Huang, C.S., Kelley, M.C., 1996b. Nonlinear evolution of equatorial spread F, 2. Gravity wave seeding of Rayleigh–Taylor instability. J. Geophys. Res. 101, 293–302.

Huba, J.D., Ossakow, S.L., 1979. On the generation of 3-m irregularities during equatorial spread F by low-frequency drift waves. J. Geophys. Res. 84, 6697–6700.

Huba, J.D., Ossakow, S.L., 1981. On 11-cm irregularities during equatorial spread F. J. Geophys. Res. 86, 829–832.

Hysell, D.L., 2000. An overview and synthesis of plasma irregularities in equatorial spread F. J. Atmos. Terr. Phys. 62, 1037–1056.

Kadomtsev, B.B., 1964. Plasma turbulence. In: Voprosi teorii plasmi, vol. 4,. Atomizdat, Moscow, p. 188 (in Russian).

Kelley, M.C., 1985. Equatorial spread F: recent results and outstanding problems. J. Atmos. Terr. Phys. 47, 745–752.

Kelley, M.C., 1989. The Earth's Ionosphere: Plasma Physics and Electrodynamics. In: International Geophysics Series, 43. Academic, San Diego, CA.

Kelley, M.C., Larson, M.F., La Hoz, C., McClure, J.P., 1981. Gravity wave initiation of equatorial spread F: a case study. J. Geophys. Res. 86, 9087–9100.

Keskinen, M.J., Szuczczewicz, E.P., Ossakow, S.L., Holmes, J., 1981. Nonlinear theory and experimental observations of the local collisional Rayleigh–Taylor instability in a descending equatorial spread F ionosphere. J. Geophys. Res. 86, 5785.

Keskinen, M.J., Ossakow, S.L., 1982. Nonlinear evolution of convecting plasma enhancements in the auroral ionosphere, 1. Long-wavelength irregularities. J. Geophys. Res. 87, 144.

Kolmogorov, A.N., 1941. The local structure of turbulence in incompressible viscous fluids for very high Reynolds numbers. Dokl. Acad. Nauk SSSR 30, 301–304.

LaBelle, J., Kelley, M.C., Seyler, C.E., 1986. An analysis of the role of drift waves in equatorial spread. J. Geophys. Res. 91, 5513–5525.

Mareev, E.A., Iudin, D.I., Molchanov, O.A., 2002. Mosaic source of internal gravity waves associated with seismic activity. In: Hayakawa, M., Molchanov, O. (Eds.), Seismo-Electromagnetics (Lithosphere–Atmosphere–Ionosphere Coupling). TERRUPUB, Tokyo, pp. 335–343.

Molchanov, O.A., Hayakawa, M., Afonin, V.V., Akentieva, O.A., Mareev, E.A., 2002. Possible influence of seismicity by gravity waves on ionospheric equatorial anomaly from data of IK-24 satellite, 1. Search for idea of seismo-ionosphere coupling, 2. Equatorial anomaly and small-scale ionospheric turbulence. In: Hayakawa, M., Molchanov, O. (Eds.), Seismo-Electromagnetics (Lithosphere–Atmosphere–Ionosphere Coupling). TERRUPUB, Tokyo, pp. 275–297.

Molchanov, O.A., Akentieva, O.S., Afonin, V.V., Mareev, E.A., Fedorov, E.N., 2003a. Plasma density-electric field turbulence in the low-latitude ionosphere from observation on satellites, possible connection with seismicity (this issue).

Molchanov, O.A., Schekotov, A.Yu., Fedorov, E.N., Belyaev, G.G., Solovieva, M., Hayakawa, M., submitted. Preseismic ULF effect and possible interpretation. Ann. Geophys.

Ossakow, S.L., 1981. Spread F theories—A review. J. Atmos. Terr. Phys. 43, 437.

Sekar, R., Kelley, M.C., 1998. On the combined effects of vertical shear and zonal electric field patterns on nonlinear equatorial spread F evolution. J. Geophys. Res. 103, 20735.

Sperling, J.L., Goldman, S.R., 1980. Electron collisional effects on lower hybrid drift instabilities in the ionosphere. J. Geophys. Res. 85, 3494–3498.

Sudan, R.N., Keskinen, M.J., 1984. Unified theory of the power spectrum of intermediate wavelength ionospheric electron density fluctuations. J. Geophys. Res. 89, 9840.

Tramutoli, V., Bello, D., Pergola, G.N., Piscitelli, S., 2001. Robust satellite technique for remote sensing of seismically active areas. Ann. Geofis. 44, 295–312.

Tronin, A., Hayakawa, M., Molchanov, O., 2002. Thermal IR satellite data application for earthquake research in Japan and China. J. Geodyn. 33, 519–534.

Tsitovich, V.N., 1967. Nonlinear Effects in Plasma. Nauka, Moscow. p. 254 (in Russian).